

# An extra $Z'$ gauge boson as a source of Higgs particles

J. Lorenzo Díaz-Cruz<sup>1</sup>, Javier M. Hernández-López<sup>1</sup> and Javier A. Orduz-Ducua<sup>1</sup>

<sup>1</sup> *Facultad de Ciencias Físico-Matemáticas,  
Benemérita Universidad Autónoma de Puebla, Puebla, México*

## Abstract

Models with extra gauge bosons often require an extended Higgs sector, which contains a rich spectrum of Higgs bosons with properties that deviate from the Standard Model (SM). Such Higgs bosons could be searched using standard mechanisms similar to the SM. However, the existence of the new gauge bosons could provide new production mechanisms, which could probe the non-standard origin of the Higgs particle. In this paper we study how the  $Z'$  from a model with extra  $U(1)'$  could be used as a source of Higgs bosons. We study 3-bodies decays of the  $Z'$  into a Higgs boson and a top anti-top pair or WW pair, namely  $Z' \rightarrow t\bar{t}h, WW h$ . We find that it is possible to get  $\mathbf{Br}'$ 's as high as  $10^{-2}$  for these modes, which could be studied at future colliders. We also study the production of the Higgs bosons in association with the  $Z$  vector boson at a linear collider, through the reaction  $e^+e^- \rightarrow Z, Z' \rightarrow Z + h$ , including both the resonant and the non-resonant effects.

# 1 Introduction

After many years of preparation, the LHC has tested in very significant ways the Higgs sector of the SM. In fact the LHC announcement of the discovery of a new boson, with properties that resemble those of the SM Higgs boson can be considered a great triumph of particle physics. The new boson has a mass  $m_h \simeq 125$  GeV [1, 2], which agrees quite well with the range preferred by the analysis of electroweak precision tests. The LHC has also searched for new physics beyond the SM, and so far only has extended the bounds on the new physics scale.

Some of the simplest extensions of the SM are those that add new gauge bosons, which could arise from a variety of contexts, ranging from simple extra  $U(1)$  gauge symmetries [3], left-right models [3, 4, 5, 6], GUTs [7], and even string theory [8, 9, 10]. In particular, extension of the SM with an extra  $U(1)'$  have been studied extensively, including the detection at LHC, as well as other phenomenological aspects [3, 4, 5, 6, 7, 8, 9, 10].

The crucial test for this kind of models is precisely the presence of new  $Z'$  gauge boson, and recent bounds from LHC indicate that it should be heavier than about 1.5 TeV[11, 12, 13]. Future LHC runs at 13-14 TeV will increase the  $Z'$  mass bounds or luckily will find evidence of its presence. Further studies will require a new linear collider, which will also allow us to perform precision studies of the Higgs sector, in order to search for the nature of the Higgs mechanism at more fundamental level.

The Higgs boson from these models could be searched using mechanisms similar to the SM one. However, the existence of such new gauge bosons could also provide new Higgs production mechanisms, which could probe its non-standard origin. In this paper we are interested in studying how the  $Z'$  from a model with extra  $U(1)'$ , could be used as a source of Higgs bosons. We calculate the decay widths for the 3-body decays of the  $Z'$  into a Higgs boson, namely for  $Z' \rightarrow t\bar{t}h, WW_h$ . We find that it is possible to get  $\mathbf{Br}$ 's as high as  $10^{-2}$  for these modes, which could be studied at LHC. We also calculate the production of the Higgs bosons in association with the  $Z$  vector boson at a linear collider, i.e.  $e^+e^- \rightarrow Z, Z' \rightarrow Z + h$ , with  $Z'$  either on-shell

or off-shell.

The organization of this paper goes as follows: section 2 contains a summary of the  $U(1)_{B-L}$  model with extra  $Z'$ . Then, section 3 includes the calculation of the 3-body decays of  $Z'$  into a Higgs boson and a pair of SM particles,  $Z' \rightarrow t\bar{t}h, WW h$ . Section 4 contains our calculation of  $e^+e^- \rightarrow Z, Z' \rightarrow Z + h$ , while Section 5 includes our conclusions. Some of the lengthy formulae appearing in the calculation of the 3-body decays are included in the appendices.

## 2 A $U(1)_{B-L}$ model with extra $Z'$ : parameters and bounds

In this section we will describe the Lagrangian, including the gauge and fermionic sectors for  $SU(2)_L \times U(1)_Y \times U(1)'$  model, we also write the Higgs potential and the Higgs coupling. The gauge sector is given by [14, 15],

$$\mathcal{L}_g = -\frac{1}{4}B_{\mu\nu}B^{\mu\nu} - \frac{1}{4}W_{\mu\nu}^a W^{a\mu\nu} - \frac{1}{4}Z'_{\mu\nu}Z'^{\mu\nu} \quad (1)$$

We ignore the  $SU(3)$  sector for the purposes of the paper. The field strength tensor are labeled as  $W_{\mu\nu}^a, B_{\mu\nu}$  and  $Z'_{\mu\nu}$  for  $SU(2)_L, U(1)_Y$  and  $U(1)'$ , respectively. We need to transform eq.(1) in order to obtain the physical mass eigenstates [16, 17].

For the scalar sector we have,

$$\mathcal{L}_s = (D^\mu\Phi)^\dagger(D_\mu\Phi) + (D^\mu\chi)^\dagger(D_\mu\chi) - V(\Phi, \chi)$$

where  $\Phi$  denotes the SM scalar doublet and  $\chi$  is a singlet under the SM. The covariant derivate for a pure  $B - L$  model is [18, 19, 20],

$$D_\mu = \partial_\mu + i [gT^a W_\mu^a + g_1 Y B_\mu + g' Y' B'_\mu]$$

The doublet and singlet scalars are further written as,

$$\Phi = \begin{pmatrix} G^\pm \\ \frac{v+\phi^0+iG_Z}{\sqrt{2}} \end{pmatrix}, \quad \chi = \frac{v' + \phi'^0 + iz'}{\sqrt{2}} \quad (2)$$

In this way,  $G^\pm, G_Z$  and  $z'$  become the Goldstone bosons of  $W^\pm, Z$  and  $Z'$ , respectively. The potential that does this is [20],

$$V(\Phi, \chi) = -m^2 \Phi^\dagger \Phi - \mu^2 |\chi|^2 + \lambda_1 (\Phi^\dagger \Phi)^2 + \lambda_2 |\chi|^4 + \lambda_3 \Phi^\dagger \Phi |\chi|^2$$

After SSB we obtain the mass matrix for the neutral CP-even states,  $\phi^0$  and  $\phi'^0$ . Then, we need to diagonalize this mass matrix to obtain the mass eigenstates, i.e.

$$\begin{pmatrix} h \\ H \end{pmatrix} = \begin{pmatrix} \cos \alpha & -\sin \alpha \\ \sin \alpha & \cos \alpha \end{pmatrix} \begin{pmatrix} \phi^0 \\ \phi'^0 \end{pmatrix} \quad (3)$$

Where  $\alpha$  is the mixing angle for the neutral Higgs bosons. However in order to respect the recent constraints from LHC on the Higgs couplings[1, 2] we shall fix the mixing angle to be  $\cos \alpha \simeq 1$ , i.e.  $h \simeq \phi^0$ .

The couplings of a  $Z'$  boson to the SM fermions are given by,

$$\mathcal{L}_{NC} = g_{Zff} \sum_f \bar{f} \gamma^\mu \left( g_V^f + g_A^f \gamma^5 \right) f Z_\mu + g_{Z'ff} \sum_f \bar{f} \gamma^\mu \left( g_V^{\prime f} + g_A^{\prime f} \gamma^5 \right) f Z'_\mu \quad (4)$$

where  $g_{Zff} = \frac{g}{\cos \theta_W}$ ,

$$\begin{aligned} g_V^f &= \frac{T_3^f}{2} \cos \theta' - Q^f \cos \theta' \sin^2 \theta_W - \frac{g'}{2g_1} \sin \theta' \sin \theta_W, \\ g_A^f &= -\frac{T_3^f}{2} \cos \theta' \cos^2 \theta_W \end{aligned} \quad (5)$$

and

$$\begin{aligned} g_V^{\prime f} &= \frac{T_3^f}{2} \sin \theta' - Q^f \sin \theta' \sin^2 \theta_W + \frac{g'}{2g_1} \cos \theta' \sin \theta_W, \\ g_A^{\prime f} &= -\frac{T_3^f}{2} \sin \theta' \cos^2 \theta_W \end{aligned} \quad (6)$$

As it is given in the SM  $\frac{g_1}{g} = \frac{\sin \theta_W}{\cos \theta_W}$ . Similarly, in the forthcoming calculations we will use the following definitions the couplings for gauge and neutral Higgs bosons which are shown in table (1).

Table 1: Definitions for vertices with gauge and Higgs boson.

$g_{ZWW}$	$g_{Z'WW}$
$ig \cos \theta' \sin \theta_W$	$ig \sin \theta' \sin \theta_W$

and

$$g_{hZZ'} = \frac{1}{4} \frac{v}{M_W} \left[ f(\theta') \cos \alpha - g(\theta') \sin \alpha \right]$$

where  $f(\theta') = \sin 2\theta' (g^2 + g_1^2 - g'^2) + 2g' \cos 2\theta' \sqrt{g^2 + g_1^2}$ ,  $g(\theta') = 4rg'^2 \sin 2\theta'$  and  $r = \frac{v'}{v}$ . The  $Z - Z'$  mixing angle is taken as  $\theta' = 10^{-3}$  ( $\theta' = 10^{-4}$ ) which respects the currents bounds on this parameter[21]. According to recent LHC results we must take  $m_h = 125$  GeV, for the SM-like Higgs boson, the vacuum expectation value is taken as  $v' = 2$  TeV. We took the value  $\alpha = \frac{\pi}{9}$  for the Higgs mixing parameter, which is in the agreement with [1, 2, 22].

### 3 Three body decays: $Z' \rightarrow t\bar{t}h, W^+W^-h$

In the following we present the formulae for the 3-body decays of the  $Z'$  that include a Higgs boson in the final state, namely for the modes  $Z' \rightarrow t\bar{t}h$  and  $Z' \rightarrow WWh$ . Since the dominant two-body decay modes are needed in order to calculate the corresponding branching ratios (**Br**), we shall also present the explicit expressions for the corresponding decay widths.

#### 3.1 Two-body modes

The dominant decays of  $Z'$  includes the decay into a fermion pair ( $Z' \rightarrow f\bar{f}$ ), gauge boson pair ( $Z' \rightarrow W^+W^-$ ) and into a higgs and a Z boson ( $Z' \rightarrow Zh$ ).

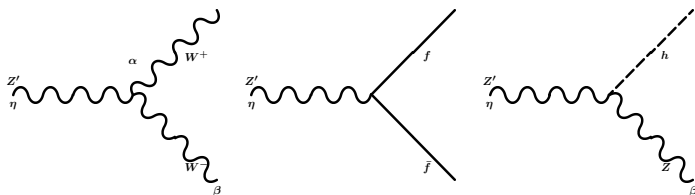


Figure 1: Feynman diagrams for two bodies

The decay width for  $Z' \rightarrow W^+W^-$  process is given by[23]:

$$\Gamma(Z' \rightarrow W^+W^-) = \frac{g_{Z'WW}^2 M_{Z'}^3}{128\pi r_W^2} (1 - 2r_W)^{1/2} (1 - 4r_W) (r_W(32r_W - 5) + 1) \quad (7)$$

where  $g_{Z'WW}$  is include in table (1) and  $r_W = \frac{M_W^2}{M_{Z'}^2}$ .

The decays width for  $Z' \rightarrow f\bar{f}$  is given by[14, 23]:

$$\Gamma(Z' \rightarrow f\bar{f}) = \frac{g_{Z'ff}^2 M_{Z'}}{4\pi} \sqrt{1 - 4r_f} \left( g_A^2 (1 - 4r_f) + g_V^2 (2r_f + 1) \right) \quad (8)$$

The coefficients  $g_{V,A}^f$  are the couplings that appear in eqs. (6) and  $r_f = \frac{m_f^2}{M_{Z'}^2}$ .

Finally, the decay width for the mode  $Z' \rightarrow Zh$  is given by[24]:

$$\Gamma(Z' \rightarrow Zh) = \frac{g_{hZZ'}^2 M_{Z'} r_{WZ}}{64\pi} \sqrt{r_h^2 - 2r_h(r_Z + 1) + (r_Z - 1)^2} \times \\ (r_h^2 - 2r_h(r_Z + 1) + r_Z(r_Z + 10) + 1) \quad (9)$$

where  $g_{hZZ'}$  is shown in table (1),  $r_{WZ} = \frac{M_W^2}{M_Z^2}$ ,  $r_h = \frac{m_h^2}{M_{Z'}^2}$  and  $r_Z = \frac{M_Z^2}{M_{Z'}^2}$ .

In general, we shall use the following notation:  $r_i = m_i^2/M_{Z'}^2$ , and  $r_{ij} = m_i^2/M_j^2$ .

### 3.2 $Z' \rightarrow f\bar{f}h$

The amplitud for the decay  $Z' \rightarrow f\bar{f}h$  procceds through the following Feynman diagrams,

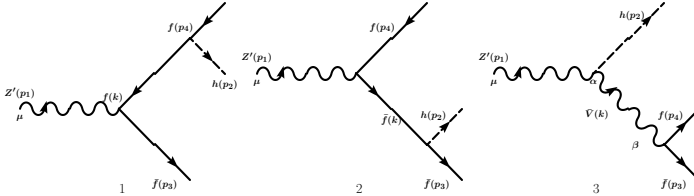


Figure 2: Feynman diagrams for three bodies with involved femions in the final state.

The corresponding invariant amplitud is given by,

$$|\overline{\mathcal{M}}_{123}|^2 = \sum_{i=1}^3 |\overline{\mathcal{M}}_i|^2 + 2 \sum_{\substack{i,j=1 \\ i \neq j}}^3 \mathbf{Re}(\overline{\mathcal{M}}_i \overline{\mathcal{M}}_j^*)$$

By performing the calculations, we obtain the following result for the differential decay width:

$$\begin{aligned}
\frac{d\Gamma(Z' \rightarrow f\bar{f}h)}{dxdy} = & \frac{M_{Z'}}{256\pi^3} \left( g_{ffh}^2 g_{Zff}^2 f_1(g_A^f, g_V^f; x, y) + \right. \\
& g_{ffh}^2 g_{Zff}^2 f_2(g_A^f, g_V^f; x, y) + g_{Zff}^2 g_{Z'h}^2 f_3(g_A^f, g_V^f; x, y) + \\
& 2 \left( g_{ffh}^2 g_{Zff}^2 f_{12}(g_A^f, g_V^f; x, y) + \right. \\
& g_{ffh} g_{Zff} g_{Zff} g_{Z'h} f_{13}(g_A^f, g_A^f, g_V^f, g_V^f; x, y) + \\
& \left. \left. g_{ffh} g_{Zff} g_{Zff} g_{Z'h} f_{23}(g_A^f, g_A^f, g_V^f, g_V^f; x, y) \right) \right) \quad (10)
\end{aligned}$$

the integration limits for the scaled energy variables  $(x, y) = (2E_h/M_{Z'}, 2E_f/M_{Z'})$  are,

$$2\sqrt{r_2} \leq x \leq 1 + r_2 - 4r_4 \quad \text{and} \quad \frac{A-B}{2C} \leq y \leq \frac{A+B}{2C}$$

where  $A = (2-x_h)(1+r_h-x)$ ,  $B = \sqrt{(x^2 - 4r_h)(1+r_h-x-4r_f)(1+r_h-x)}$  and  $C = (1-x+r_h)$ . The expressions for the functions  $f_1, f_2, f_3, f_{12}, f_{13}, f_{23}$  are shown in Appendix A.

### 3.3 $Z' \rightarrow W^+W^-h$

The Feynman diagrams that contribute to the decay  $Z' \rightarrow W^+W^-h$  are shown next:

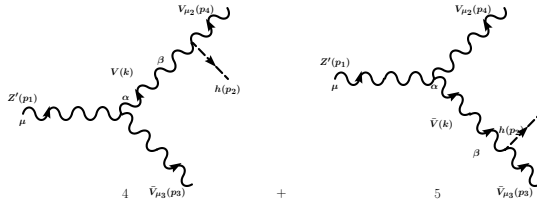


Figure 3: Feynman diagrams for three bodies with involved gauge boson in the final state.

We have performed the calculation similarly to the last subsection, including the interference terms. The resulting differential decay width is written

as:

$$\frac{d\Gamma(Z' \rightarrow W^+W^-h)}{dxdy} = \frac{M_{Z'}g_{Z'WW}^2g^2}{256\pi^3r_W} \left( f_4(x, y) + f_5(x, y) + 2f_{45}(x, y) \right) \quad (11)$$

for the definition of  $f_{4,5,45}$  see the Appendix B. The definitions for  $(x, y)$  and their integration limits, are similar to the last calculation, with  $x_f \rightarrow x_W$ .

### 3.4 Results for Br's

The recent LHC results indicate that the Higgs boson mass is  $m_h \simeq 125$  GeV [1, 2, 25], which is the nominal value we use in the following plots. We show the Branching ratio for different channels as a function of the  $Z'$  gauge boson mass. We consider the  $B - L$  scenarios for the fermion- $Z'$  couplings, with  $\theta' = 10^{-3}$  ( $\theta' = 10^{-4}$ ).

We can see from figure 5 that the  $\mathbf{Br}(Z' \rightarrow WW)$  is not dominant, because this process depends on the coupling  $g_{Z'WW}$  (eq.(7)) which decreases with  $\theta'$ . For the  $\mathbf{Br}(Z' \rightarrow f\bar{f})$  and  $\mathbf{Br}(Z' \rightarrow Zh)$ , the global factor coming from the denominator in the second process is about ten times larger than the one appearing in the first process, such that:  $\mathbf{Br}(Z' \rightarrow f\bar{f}) > \mathbf{Br}(Z' \rightarrow Zh)$ . The decay  $Z' \rightarrow t\bar{t}h$  depends directly on the couplings  $g'_V$  and  $g'_A$ , in this case we use  $g_1 \sim g'$ . The  $Z' \rightarrow WW$  depends directly on  $\theta'^2 \sim 1 \times 10^{-6}$ , so this is suppressed too. The  $Z' \rightarrow WW h$  process depends on the product  $g_{Z'WW}g_{WW h}$  and it inversely proportional too, in such way that as  $M_{Z'}$  grows then the corresponding width grows too.

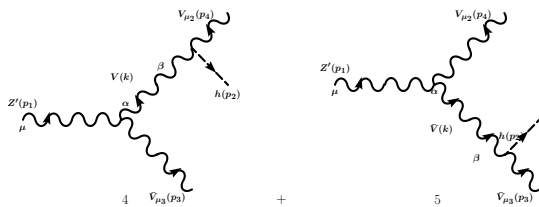


Figure 4: Feynman diagrams for three bodies with involved gauge boson in the final state.



We have performed the calculation similarly to the last subsection, including the interference terms. The resulting differential decay width is written as:

$$\frac{d\Gamma(Z' \rightarrow W^+W^-h)}{dxdy} = \frac{M_{Z'}g_{Z'WW}^2g^2}{256\pi^3r_W} \left( f_4(x, y) + f_5(x, y) + 2f_{45}(x, y) \right) \quad (12)$$

for the definition of  $f_{4,5,45}$  see the Appendix B. The definitions for  $(x, y)$  and their integration limits, are similar to the last calculation, with  $x_f \rightarrow x_W$ .

### 3.5 Results for Br's

The recent LHC results indicate that the Higgs boson mass is  $m_h \simeq 125$  GeV [1, 2, 25], which is the nominal value we use in the following plots. We show the Branching ratio for different channels as a function of the  $Z'$  gauge boson mass. We consider the  $B - L$  scenarios for the fermion- $Z'$  couplings, with  $\theta' = 10^{-3}$  ( $\theta' = 10^{-4}$ ).

We can see from figure 5 that the  $\mathbf{Br}(Z' \rightarrow WW)$  is not dominant, because this process depends on the coupling  $g_{Z'WW}$  (eq.(7)) which decreases with  $\theta'$ . For the  $\mathbf{Br}(Z' \rightarrow f\bar{f})$  and  $\mathbf{Br}(Z' \rightarrow Zh)$ , the global factor coming from the denominator in the second process is about ten times larger than the one appearing in the first process, such that:  $\mathbf{Br}(Z' \rightarrow f\bar{f}) > \mathbf{Br}(Z' \rightarrow Zh)$ . The decay  $Z' \rightarrow t\bar{t}h$  depends directly on the couplings  $g'_V$  and  $g'_A$ , in this case we use  $g_1 \sim g'$ . The  $Z' \rightarrow WW$  depends directly on  $\theta'^2 \sim 1 \times 10^{-6}$ , so this is suppressed too. The  $Z' \rightarrow WW h$  process depends on the product  $g_{Z'WW}g_{WW h}$  and it inversely proportional too, in such way that as  $M_{Z'}$  grows then the corresponding width grows too.

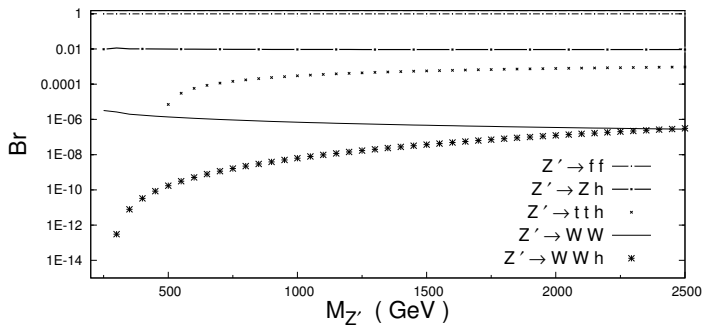


Figure 5:  $v' = 2 \text{ TeV}$ .

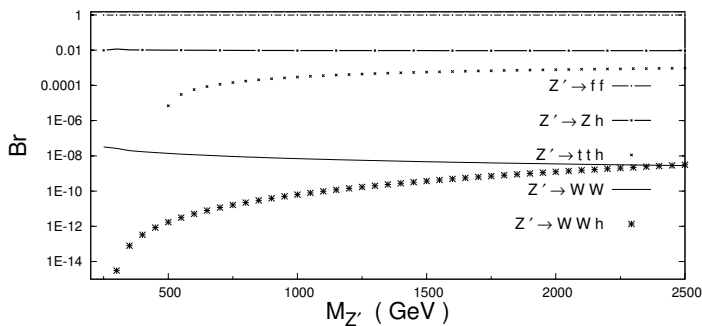


Figure 6:  $v' = 2 \text{ TeV}$ .

In fig. 5 we show the numerical results for  $\theta' = 10^{-3}$ , and for comparison we also show in fig. and 6 the corresponding ones for  $\theta' = 10^{-4}$ . We notice that there is a decrease in the decays  $Z' \rightarrow WW, WW h$ , whereas the decay  $Z' \rightarrow ff, tth$  remain essentially constant.

#### 4 The reaction $e^+e^- \rightarrow Z', Z^* \rightarrow Z + h$ at ILC

In this section we study the Higgs production at  $e^+e^-$  colliders, through the reaction  $e^+e^- \rightarrow Z, Z' \rightarrow Zh$ , taking into account the contribution of resonant ( $Z'$ ) and non-resonant effects ( $Z$ ). When  $\sqrt{s} = M_{Z'}$  one expects that the production of  $Z + h$  is dominated by the decay  $Z' \rightarrow Zh$ , however the vertex  $ZZ'h$  is suppressed by the mixing angle  $\theta'$ , and therefore it is interesting to study the contribution from the non-resonant amplitude.

The Feynman diagrams for the reaction are shown in fig. 7,

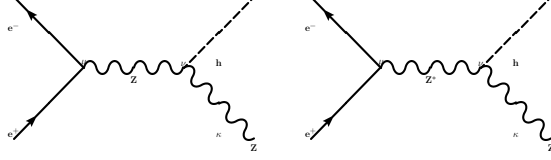


Figure 7: Feynman diagrams for  $e^+e^- \rightarrow Zh$

the total amplitude is:  $\mathcal{M} = \mathcal{M}_1 + \mathcal{M}_2$ . Where,

$$\begin{aligned}\mathcal{M}_1 &= g_{ZZ'h}g_{Zff}g^{\nu\kappa}\frac{g_{\mu\nu}}{p_{Z'}^2 - M_{Z'}^2 + iM_{Z'}\Gamma_{Z'}}\bar{u}\gamma^\mu(g_V^f + g_A^f\gamma^5)v\epsilon^{\kappa*} \\ \mathcal{M}_2 &= g_{ZZ'h}g_{Z'f\bar{f}}g^{\nu\kappa}\frac{g_{\mu\nu}}{p_{Z^*}^2 - M_Z^2 + iM_Z\Gamma_Z}\bar{u}\gamma^\mu(g_V^f + g_A^f\gamma^5)v\epsilon^{\kappa*}.\end{aligned}$$

The resulting cross section is given by,

$$\begin{aligned}\sigma(e^+e^- \rightarrow Z, Z' \rightarrow Zh) &= \frac{\left( (1 - 2\sqrt{r_h r_Z} - r_h - r_Z) (1 + 2\sqrt{r_h r_Z} - r_h + r_Z) \right)^{1/2}}{8\pi s r_{ZW} \sqrt{\frac{1}{4}(1 - 2r_f)^2 - r_f^2}} \times \\ &\left[ \frac{g_{Z'h}^2 g_{Z'f\bar{f}}^2 \left( g_A^{f2} R_{fZ} + g_V^{f2} T_{fZ} \right)}{2c_r^2 + 2r_{Z'} R_{Z'}} + \frac{g_{Zh}^2 g_{Zf\bar{f}}^2 \left( g_A^{f2} R_{fZ} + g_V^{f2} T_{fZ} \right)}{2c_r^2 + 2r_Z R_Z} + \right. \\ &\left. \frac{g_{Z'h} g_{Z'f\bar{f}} g_{Zh} g_{Zf\bar{f}} \left( c_r' c_r + \sqrt{r_{Z'} r_Z R_{Z'} R_Z} \right) \left( g_A^f g_A^f R_{fZ} + g_V^f g_V^f T_{fZ} \right)}{\left( c_r' c_r + \sqrt{r_{Z'} r_Z R_{Z'} R_Z} \right)^2 + \left( \sqrt{r_{Z'} R_{Z'}} c_r - c_r' \sqrt{r_Z R_Z} \right)^2} \right]\end{aligned}$$

where  $R_{fZ} = (4 - 32r_f)r_Z + 1$ ,  $T_{fZ} = 4(4r_f + 1)r_Z + 1$ ,  $c_r = 1 - r_Z$ ,  $c_r' = 1 - r_{Z'}$  and  $g_{Zff}$ , and  $g_{hZZ'}$  appear in eq. (5) and in table (1). In this section,

we have used  $r_i = \frac{m_i^2}{s}$ ,  $r_{ij} = \frac{m_i^2}{m_j^2}$ ,  $R_Z = \frac{\Gamma_Z^2}{s}$  and  $R_{Z'} = \frac{\Gamma_{Z'}^2}{s}$ . The  $g'_{V,A}(g_{V,A})$  are the  $Z'ff(Zff)$  couplings that appear in eq.(4).

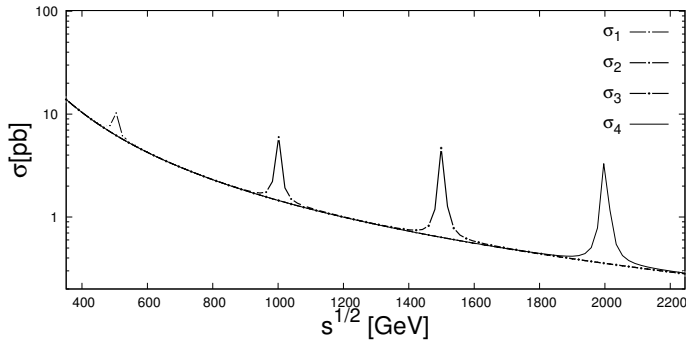


Figure 8: The cross sections for Higgs production with the  $Z'$  in resonance. We use  $v' = 2\text{ TeV}$ , the intensity in resonance decreases when we raise the value for  $v'$ .  $\sigma_{1-4}$  correspond to the cases of  $M_{Z'} = 0.5, 1, 1.5, 2\text{ TeV}$ , respectively.

We can see from the fig. 8, that when  $\sqrt{s} = M_{Z'}$ , the resonant effect dominates the Higgs production, despite the fact that the coupling  $ZZ'h$  is suppressed.

## 5 Conclusions

Models containing an extra gauge boson often include a rich spectrum of Higgs bosons, with properties that deviate from the Standard Model (SM) case. Such Higgs bosons could be searched using standard mechanisms, similar to the SM. However, the existence of such new gauge bosons could also be used to provide new production mechanisms, which could probe the non-standard origin of the Higgs couplings.

In this paper we have studied how the  $Z'$  arising from a model with a extra  $U(1)'$  could be used as a source of Higgs bosons. For such a task, we

concentrate in the  $Z' \rightarrow \bar{t}th$  channel, and we found a **Br** for this mode  $10^{-2}$  far a wide range of the parameter space, which could be within the reach for both accelerators LHC and ILC. To appreciate the importance of the resonant effect for Higgs production one can see the fig.8 when  $\gamma$  is significant.

Further, at the next linear collider (ILC) one could achieve luminosities  $\sim \mathcal{O}(\text{ab}^{-1})$  at  $\sqrt{s} \sim \mathcal{O}(\text{TeV})$  [26, 27], which could give a number of events:  $N = \sigma(e^+e^- \rightarrow Z, Z' \rightarrow Zh)_{M_{Z'}=1 \text{ TeV}} \times \mathcal{L}_{NLC} \sim 1\text{pb} \times 1\text{ab}^{-1} \sim 10^6$ , which seems feasible to be detected and it will be possible to perform precision measurements for  $Z'$  and Higgs. In models with an extra Higgs doublet, it could be possible to get larger couplings of the Higgs boson with b-quarks, and this will also allow to study the decay  $Z' \rightarrow bbh$ , which could be detectable even at LHC [28].

## Acknowledgements

We acknowledge support from CONACYT-SNI (Mexico). We thank Enrique Díaz for reading the manuscript and his comments.

## A Appendices

The next equations are used to obtain the  $\Gamma(Z' \rightarrow f\bar{f}h)$  in eq.(10),

$$\begin{aligned}
f_1(g'_A{}^f, g'_V{}^f; x, y) &= -\frac{2}{(x+y-1)^2} \left( g'^2_A \left( 32r_f^2 + 4r_f(-2r_h + x^2 + 2x(y+1) + y(y+2) - 5) + \right. \right. \\
&\quad \left. \left. (x+y)(-r_h(x+y-2) + x(x+y-3) + y) + r_h + x - 2y + 1 \right) + \right. \\
&\quad \left. g'^2_V \left( -16r_f^2 + 4r_f(r_h + x^2 + 2x(y-2) + (y-4)y + 1) + \right. \right. \\
&\quad \left. \left. (x+y)(-r_h(x+y-2) + x(x+y-3) + y) + r_h + x - 2y + 1 \right) \right) \\
f_2(g'_A{}^f, g'_V{}^f; x, y) &= \frac{2}{(y-1)^2} \left( g'^2_V \left( r_h(8r_f + (y-2)y - 1) - (y-1)(xy + x + y - 1) \right) \right. \\
&\quad \left. - g'^2_A \left( r_h(4r_f - (y-2)y + 1) + (y-1)(xy + x + y - 1) \right) \right)
\end{aligned}$$

$$f_3(g_A, g_V; x, y) = \frac{2r_W}{(-r_h + r_Z + x - 1)^2} \left( g_V^2 (4r_f + r_h - xy - x - y^2 + 2y + 1) - g_A^2 (8r_f - r_h + (x - 2)y + x + y^2 - 1) \right)$$

and the interference terms,

$$f_{12}(g_A^f, g_V^f; x, y) = \frac{2}{(y - 1)(x + y - 1)} \left( g_A^2 (2r_f(4r_h + (x + 4)y + x - 4) - 2r_h^2 - r_h(x(y - 3) + (y - 1)^2) + (x + 1)(y - 1)(x + y - 1)) + g_V^2 (2r_f(-4r_h + x^2 + (x - 2)y + x + 2) + 2r_h^2 + r_h(x(y - 3) + (y - 1)^2) - (x + 1)(y - 1)(x + y - 1)) \right)$$

$$f_{13}(g_A, g_A^f, g_V, g_V^f; x, y) = -\frac{2\sqrt{r_f}\sqrt{r_W}}{(x + y - 1)(-r_h + r_Z + x - 1)} \left( g_A g_A^f (16r_f + 2y^2 - 4r_h + 3xy + x(x + 3) - 6) + g_V g_V^f (2r_h + (x + y - 3)(x + 2y) - 8r_f) \right)$$

$$f_{23}(g_A, g_A^f, g_V, g_V^f; x, y) = \frac{2\sqrt{r_f}\sqrt{r_W}}{(x + y - 1)(r_h - r_Z - x + 1)} \left( g_A g_A^f (2r_h + (x + 4)y + x - 4) + g_V g_V^f (-4r_h + (x - 2)y + x + 2) \right)$$

## B Appendices

The next equations are used to obtain the  $\Gamma(Z' \rightarrow W^+W^-h)$  in eq.(12),

$$f_4(x, y) = \frac{1}{4(x + y - 1)^2} \left( 4(x - y - 14)r_W^3 + 4(3y^2 + 6xy - 20y + 2(x - 5)x + 17)r_W^2 + (x^3 + (3y - 2)x^2 + (y - 1)(7y - 3)x + (y - 1)^2(5y - 14))r_W + (x - y + 1)(y - 1)^2 - r_h^2(y - x^2 + x + r_W(x - y + 2) - 1) + 2r_h(8r_W^2 - (y^2 + 3xy - 7y + x(2x - 7) + 6)r_W - (y - 1)^2) \right)$$

$$f_5(x, y) = \frac{1}{16(y - 1)^2} \left( 8r_h^3 + (x^2 + 4(2y - 3)x + 16(y - 1)^2 + r_W(-8x + 8y - 52))r_h^2 + 2(8(x - y + 7)r_W^2 - 4(y - 1)(3x + 6y - 7)r_W - (x^2 + 4(y - 1)x + 4(y - 1))(y - 1))r_h + x(x + 4)(y - 1)^2 + 16r_W^3(x - y - 14) - 8r_W^2(x^2 - 4x - 8y^2 + 14y - 6) + 4r_W((2y - 1)x^2 + 4(y - 1)yx + (y - 1)^2(2y - 1)) \right)$$

and

$$\begin{aligned}
f_{45}(x, y) = & -\frac{1}{8(-2r_h + 2r_W + y - 1)(x + y - 1)} \left( r_h^3 + \left( x^2 + 4yx + 2r_W(x - y - 8) + \right. \right. \\
& 3(1 - 2x - y) r_h^2 + \left( 4(y - x + 22)r_W^2 - (5x^2 + 16yx - 24x + 12y^2 - 40y + 28) r_W - \right. \\
& (y - 1)(x^2 + 5y - 5) \left. \right) r_h + (2x - y + 1)(y - 1)^2 + 8r_W^3(x - y - 14) + 4r_W^2 \left( 7y^2 - 27y + \right. \\
& \left. \left. x(6y - 8) + 20 \right) + r_W \left( x^3 + (5y - 3)x^2 + (6y^2 - 4y - 2)x + 6(y - 2) \right) \right)
\end{aligned}$$

## References

- [1] Serguei Chatrchyan et al. Observation of a new boson at a mass of 125 GeV with the CMS experiment at the LHC. *Phys.Lett.*, B716:30–61, 2012.
- [2] Georges Aad et al. Observation of a new particle in the search for the Standard Model Higgs boson with the ATLAS detector at the LHC. *Phys.Lett.*, B716:1–29, 2012.
- [3] Jogesh C. Pati and Abdus Salam. Lepton Number as the Fourth Color. *Phys.Rev.*, D10:275–289, 1974.
- [4] Rabindra N. Mohapatra and Jogesh C. Pati. Left-Right Gauge Symmetry and an Isoconjugate Model of CP Violation. *Phys.Rev.*, D11:566–571, 1975.
- [5] Rabindra N. Mohapatra and Goran Senjanovic. Neutrino Masses and Mixings in Gauge Models with Spontaneous Parity Violation. *Phys.Rev.*, D23:165, 1981.
- [6] Rabindra N. Mohapatra and Goran Senjanovic. Neutrino Mass and Spontaneous Parity Violation. *Phys.Rev.Lett.*, 44:912, 1980.
- [7] Gordon L. Kane. Perspectives on supersymmetry. 1998.
- [8] Mirjam Cvetič and Paul Langacker. Implications of Abelian extended gauge structures from string models. *Phys.Rev.*, D54:3570–3579, 1996.

- [9] Mirjam Cvetič and Paul Langacker. New gauge bosons from string models. *Mod.Phys.Lett.*, A11:1247–1262, 1996.
- [10] G. Cleaver, Mirjam Cvetič, J.R. Espinosa, L.L. Everett, P. Langacker, et al. Physics implications of flat directions in free fermionic superstring models. 2. Renormalization group analysis. *Phys.Rev.*, D59:115003, 1999.
- [11] Paul Langacker. The Physics of Heavy  $Z'$  Gauge Bosons. *Rev.Mod.Phys.*, 81:1199–1228, 2009.
- [12] Ross Diener, Stephen Godfrey, and Travis A.W. Martin. Discovery and Identification of Extra Neutral Gauge Bosons at the LHC. 2009.
- [13] Ken Hsieh, Kai Schmitz, Jiang-Hao Yu, and C.-P. Yuan. Global Analysis of General  $SU(2) \times SU(2) \times U(1)$  Models with Precision Data. *Phys.Rev.*, D82:035011, 2010.
- [14] A. Ferroglia, A. Lorca, and J.J. van der Bij. The  $Z'$  reconsidered. *Annalen Phys.*, 16:563–578, 2007.
- [15] Thomas G. Rizzo.  $Z'$  phenomenology and the LHC. pages 537–575, 2006.
- [16] Robert Foot and Xiao-Gang He. Comment on  $Z$   $Z'$ -prime mixing in extended gauge theories. *Phys.Lett.*, B267:509–512, 1991.
- [17] K.S. Babu, Christopher F. Kolda, and John March-Russell. Implications of generalized  $Z$  -  $Z'$ -prime mixing. *Phys.Rev.*, D57:6788–6792, 1998.
- [18] Lorenzo Basso, Alexander Belyaev, Stefano Moretti, Giovanni Marco Pruna, and Claire H. Shepherd-Themistocleous.  $Z'$  discovery potential at the LHC in the minimal  $B - L$  extension of the Standard Model. *Eur.Phys.J.*, C71:1613, 2011.
- [19] Lorenzo Basso, Stefano Moretti, and Giovanni Marco Pruna. Constraining the  $g'_1$  coupling in the minimal  $B - L$  Model. *J.Phys.G*, G39:025004, 2012.



- [20] Lorenzo Basso, Stefano Moretti, and Giovanni Marco Pruna. A Renormalisation Group Equation Study of the Scalar Sector of the Minimal B-L Extension of the Standard Model. *Phys.Rev.*, D82:055018, 2010.
- [21] J. Beringer et al. *Phys. Rev.*, D86:010001, 2012.
- [22] Amit Chakraborty, Biswaranjan Das, J.Lorenzo Diaz-Cruz, Dilip Kumar Ghosh, Stefano Moretti, et al. The 125 GeV Higgs signal at the LHC in the CP Violating MSSM. 2013.
- [23] A. Leike. The Phenomenology of extra neutral gauge bosons. *Phys.Rept.*, 317:143–250, 1999.
- [24] Tomohiro Abe, Tatsuya Masubuchi, Shoji Asai, and Junichi Tanaka. Drell-Yan Production of  $Z'$  in the Three-Site Higgsless Model at the LHC. *Phys.Rev.*, D84:055005, 2011.
- [25] Jens Erler. Weighing in on the Higgs. 2012.
- [26] Frank Simon. Prospects for Precision Higgs Physics at Linear Colliders. 2012.
- [27] Ruo-Cheng Jiang, Xiao-Zhou Li, Wen-Gan Ma, Lei Guo, and Ren-You Zhang. Triple  $Z^0$ -boson production in large extra dimensions model at ILC. *Chin.Phys.Lett.*, 29:111101, 2012.
- [28] C. Balazs, J.L. Diaz-Cruz, H.J. He, Timothy M.P. Tait, and C.P. Yuan. Probing Higgs bosons with large bottom Yukawa coupling at hadron colliders. *Phys.Rev.*, D59:055016, 1999.